Simulation and optimization of night cooling with diffuse ceiling ventilation and mixing ventilation in a cold climate

Guo, Rui; Hu, Yue; Heiselberg, Per; Johra, Hicham; Zhang, Chen; Peng, Pei

Published in:
Renewable Energy

DOI (link to publication from Publisher):
10.1016/j.renene.2021.07.077

Publication date:
2021

Document Version
Publisher's PDF, also known as Version of record

Renewable Energy 179 (2021) 488–501

Contents lists available at ScienceDirect

Renewable Energy

journal homepage: www.elsevier.com/locate/renene

Simulation and optimization of night cooling with diffuse ceiling ventilation and mixing ventilation in a cold climate

Rui Guo *, Yue Hu , Per Heiselberg , Hicham Johra , Chen Zhang , Pei Peng

Department of the Built Environment, Aalborg University, Thomas Manns Vej 23, Aalborg, 9220, Denmark

ARTICLE INFO

Article history:
Received 18 March 2021
Received in revised form
2 July 2021
Accepted 17 July 2021
Available online 18 July 2021

Keywords:
Night ventilation
Convective heat transfer coefficient
Mixing ventilation
Diffuse ceiling ventilation
Building energy simulation
Optimization

ABSTRACT

Accurate convective heat transfer coefficient (CHTC) is crucial to assess the night ventilation performance accurately. Previous experimental studies proposed CHTC correlations tailored for night cooling with diffuse ceiling ventilation (DCV) and mixing ventilation (MV). A holistic approach integrating the building energy simulation and optimization method was put forward to validate the experimentally proposed correlations, simulate and optimize the performance of night cooling with DCV and MV. The validation results demonstrated that the proposed correlations predicted the surface temperatures accurately with a maximum mean absolute error of 1.9 °C. For a typical air-conditioned office room, night cooling with DCV saved about 0.2 kWh/m^2 total cooling energy per unit floor area (TCEC) more and provided a lower average predicted percentage of dissatisfied during the working hours (aPPD) by up to 3.1% than that with MV. Compared with the validated correlations, the empirical ceiling diffuser convection algorithm overestimated the night energy-saving potential by up to 0.5 kWh/m^2 (13.8%) and yielded a maximum difference in the aPPD of 1.5%. Optimization significantly saved TCEC by 1.1 kWh/m^2 (29.0%) for DCV and 0.9 kWh/m^2 (25.7%) for MV while maintaining the aPPD within 10%, compared to respective base cases.

1. Introduction

1.1. Background

Overheating is an ever-growing problem in buildings, especially for office buildings. It induces massive cooling demands in buildings, which is a serious challenge at the design stage and during operation [1]. Night ventilation (NV) is a promising and effective passive cooling technique to alleviate this problem. It consists of ventilating the indoor environment by natural or mechanical means to cool down the indoor thermal mass. The cooled building can then act as a heat sink during the next daytime to reduce the cooling demand and improve thermal comfort during the warmer daytime [2]. Building energy simulation (BES) tools allow the architects or engineers to evaluate or predict the NV performance for decision making. However, they are still hesitant to adopt NV due to the high uncertainty of performance prediction. NV performance is dependent on many factors [3,4], of which convective heat transfer coefficient (CHTC) and thermal mass level were two crucial parameters [5]. Moreover, the air distribution principles also impact the night cooling effectiveness [6].

Over the past half-century, numerous experimental studies have investigated the CHTC correlations for calculating the CHTC for different facing surfaces under various zone airflow regimes and heat flow directions [7]. Some of those correlations have been implemented in BES tools such as EnergyPlus [8]. People can select a convection algorithm (i.e., a set of correlations for different surfaces) for a zone or set the custom correlation for the specific surface in BES tools. Goethals et al. [9] stated that the appropriate selection of empirical correlations for a night-cooled room was imperative. NV removes excess heat by convection. A high air change rate per hour (ACH) up to 10 h^{-1} or more if applicable can thus be employed, especially for office buildings usually unoccupied at night [2]. The CHTC thus plays an important role in estimating NV performance. The existing empirical correlations were mainly developed based on the steady flat plate or steady full-scale experiments. They were only applicable to specific conditions (e.g., ventilation modes, airflow regimes), which may result in a large error in predicting NV performance. Two prior studies conducted dynamic full-scale experiments to investigate the convective heat transfer of NV with displacement and mixing ventilation (MV) [10,11]. Then the heat transfer of wall-mounted attached ventilation [12,13] was investigated recently. Nevertheless, those studies focused more on the convective heat flow or CHTC instead of developing CHTC correlations for BES. Moreover, the prediction

* Corresponding author.
E-mail address: rgu@build.aau.dk (R. Guo).

https://doi.org/10.1016/j.renene.2021.07.077

Nomenclature

Latin symbols

A	Area
C	Constant
h	Convective heat transfer coefficient
k	Index of selected cases
m_i	Measured data points for each model instance i
N_p	Number of data points at interval p
r	Fraction of maximum flow rate
s_i	Simulated data points for each model instance i

Acronyms

aPPD	Average predicted percentage of dissatisfied during the working hours
AC	Air conditioner or air conditioning
ACH	Air change rate per hour
BES	Building energy simulation
CHTC	Convective heat transfer coefficient
DCV	Diffuse ceiling ventilation
HVAC	Heating, ventilation and air conditioning
MAE	Mean absolute error
MV	Mixing ventilation
NV	Night ventilation
TARP	Thermal analysis research program
TCEC	Total cooling energy use
TMY3	Typical meteorological year

discrepancy of NV performance due to the accurate correlations and other empirical correlations has rarely been studied.

Thermal mass activation is another main factor that affects NV performance. The activated thermal capacity of the indoor environment determines the amount of excess heat stored during the daytime and then released at night by ventilation [14]. Several studies experimentally [15,16] or numerically [17,18] investigated the performance of night cooling when coupled with the general thermal mass material in furniture or building elements. Leenknegt et al. [17] disclosed that the number of overheating hours was highly sensitive to selecting the CHTC and thermal mass exposure. Phase change material (PCM) with NV has gained many interests in recent years [19–23]. However, the CHTC between the thermal mass and cold supply air was ignored or derived from the empirical correlations.

There are different air distribution principles, such as MV, diffuse ceiling ventilation (DCV), and stratum ventilation [24]. MV is the most widely used ventilation concept to cool/heat the room by directly supplying the air with high momentum [24]. DCV is a relatively new air distribution principle that supplies the air to a plenum before air diffuses through the suspended ceiling panel into the occupied zone [25]. DCV allows to supply the low-temperature outdoor or conditioned air with a lower risk of draught due to the low momentum supply from the diffuse ceiling [26]. DCV was expected to have a large night cooling potential, but only two studies focused on the heat transfer in the plenum with DCV [27,28]. Moreover, BES with DCV in buildings is not yet seen in the literature [29]. Only Yu et al. [30] used a BES tool (BSim) to simulate the energy use of a room with DCV and thermally activated building systems in the ceiling slab. The convection algorithms selected for this system were not indicated. Furthermore, prior studies about air distribution principles mainly focused on ventilation effectiveness, indoor thermal comfort, and energy performance during the occupied hours [31]. Few previous studies investigated the performance of night cooling with different air distribution principles in BES tools.

Based on this research gap of NV in terms of CHTC correlation, thermal mass activation, and air distribution principles, Guo et al. conducted dynamic full-scale experiments to investigate the CHTC correlations for night cooling with mixing ventilation (MV) [32] and diffuse ceiling ventilation (DCV) [33] under various thermal mass distribution. It was found that increasing the thermal mass level of one surface can significantly augment the CHTC at this surface. Therefore, the impact of thermal mass activation on CHTC should be taken into account when assessing the NV performance. However, the CHTC correlations for the plenum and suspended diffuse ceiling were not investigated due to the restricted experimental conditions and the complex heat transfer through the suspended ceiling panel. Moreover, the experimentally proposed CHTC correlations need validation in BES tools before simulating the NV performance.

BES allows users to optimize the design of NV to improve its performance. Most previous studies applied the parametric simulation that involved a few variables with discrete values for optimization, which may not provide the global optimal solution [34–37]. Whereas, recent developments in computing have heightened the need for adopting the optimization algorithm with BES to improve the building energy performance. Cristina et al. [38] utilized the hybrid generalized pattern search algorithm with particle swarm optimization algorithm to identify the optimum PCM melting temperature in the external building envelope components. Guo et al. leveraged the Non-dominated sorting genetic algorithm II [39] to optimize the design parameters related to the cool roof and night ventilation and the evolutionary optimization [40] algorithm to optimize the parameters associated with night mechanical ventilation for an air-conditioned room. Nevertheless, they did not consider the daytime AC temperature setpoint that also determined the daytime cooling energy use, indoor thermal comfort, and the excess heat stored that NV can remove. Moreover, the CHTC correlations in those studies were from the existing empirical correlations or not indicated, which also limited the validity of their results.

1.2. Novelty and main contributions

Regarding the current state-of-the-art, this study expanded the scope of previous work [32,33], where CHTC correlations for night cooling with DCV and MV were proposed by experimental investigation. A holistic approach integrating the building energy simulation (BES) and optimization method was put forward to explore and improve the night cooling performance in this study. The proposed CHTC correlations were further validated in BES using EnergyPlus. For night cooling with DCV, the correlations for the plenum and diffuse ceiling were identified and developed using the holistic approach. Based on the validated correlations, the performance of night cooling with DCV and MV were simulated and compared. The prediction discrepancy between the validated correlations and existing empirical correlations was also evaluated. The optimal designs of night cooling with DCV and MV were finally investigated by taking into account the energy use and indoor thermal comfort.

The original contributions are briefly summarized as follows: (1) The CHTC correlations for night cooling with DCV and MV were validated, allowing the architects or engineers to accurately access the night cooling potential. (2) The performance difference between the night cooling with those two air distribution principles

and the performance prediction discrepancy between the validated correlations and existing empirical correlations were fully evaluated. (3) The night venting duration, airflow rate, minimum night indoor temperature setpoint, thermal mass activation, and daytime cooling setpoint were comprehensively optimized, supporting architects or engineers' optimal decision-making.

2. Research framework

A holistic approach was put forward to validate the proposed CHTC correlations from previous experiments, simulate and optimize the performance of night cooling with DCV and MV in terms of energy and thermal comfort (see Fig. 1). In the first step (panel b), the guarded hot box model with DCV and MV principles was built in EnergyPlus according to the experiment platform (panel a) [32,33]. The proposed correlations were then adopted in those models for validation by comparing the measured and simulated results. Moreover, before validating the proposed correlations for DCV, the correlations for the plenum were identified based on the existing convection algorithms in EnergyPlus by comparing the measured and simulated results. And the correlation for the diffuse ceiling was developed using the optimization method with the genetic algorithm to minimize the discrepancy between measured and simulated results (objective 1). In the second step (panel c), a typical office room was selected and employed with DCV and MV to investigate the performance of night cooling with DCV and MV. In the third step (panel d), parameters related to night cooling performance were optimized with the genetic algorithm to minimize the cooling energy use (objective 2) while maintaining the indoor thermal comfort within a certain level (constraint). The optimization method was enabled by integrating EnergyPlus with MATLAB, which was further described in Appendix A.

3. Validation of proposed CHTC correlations

3.1. The guarded hot box model

The guarded hot box model was built in EnergyPlus based on the real experimental platform that was further described in Appendix B. Fig. 2 shows the model that involves the plenum, room, and guarding zone as well as the principles of DCV and MV. A variable air volume (VAV) air conditioner (AC) was equipped to supply the conditioned air to the plenum (for DCV) or the room (for MV) and exhaust the air from the room (see Fig. 3). The inlet and outlet positions in Figs. 2 and 3 originated from the previous experimental setup [32,33]. While in EnergyPlus, the inlet and outlet positions were not modeled since BES tools usually assume the air is perfectly mixed in the thermal zone. Therefore, the selection of CHTC correlations for each interior surface affects the convective heat transfer of surfaces. The guarding zone was conditioned by an ideal load air conditioner (AC), which was neglected in Fig. 3. The VAV AC system consists of a VAV fan, a multi-speed direct expansion cooling coil with two speeds, an electric heating coil, an air terminal unit with single ducts, and a VAV damper. The specification of the VAV fan is further introduced in Section 4.1. The low and high speed gross rated cooling coefficient of performance of the two-speed direct expansion cooling coil is 3 and 4.5, respectively. The electric heating coil with an efficiency of 1 served as a supplementary heating component. A sizing factor 1.2 was adopted for auto-sizing the nominal capacity of coils.

The proposed correlations in Appendix B were set for the corresponding surfaces in the model. The thermal zone in EnergyPlus only exchanges energy with the inside of the internal mass (e.g., furniture) [8]. Therefore, for design cases with four indoor tables, eight internal masses were set in the room. Each internal mass was made up of one 18 mm fiber plasterboard to represent one indoor table's surface. Finally, the model was simulated based on experimental design cases to output the simulated results. The mean absolute error (MAE) given by Eq. (1) was selected to compare the measured and simulated results.

$$MAE\ (\%) = \frac{1}{N_p} \sum_{i=1}^{N_p} (m_i - s_i) \tag{1}$$

where m_i and s_i are the measured and simulated data points for each model instance$i$, respectively. N_p is the number of data points at interval p (i.e., 480 points from 8h data with a 1-min interval). To validate the proposed correlations for DCV and MV, the measured and simulated temperatures of interior surfaces and tables were compared. Before validating the correlations for DCV, the

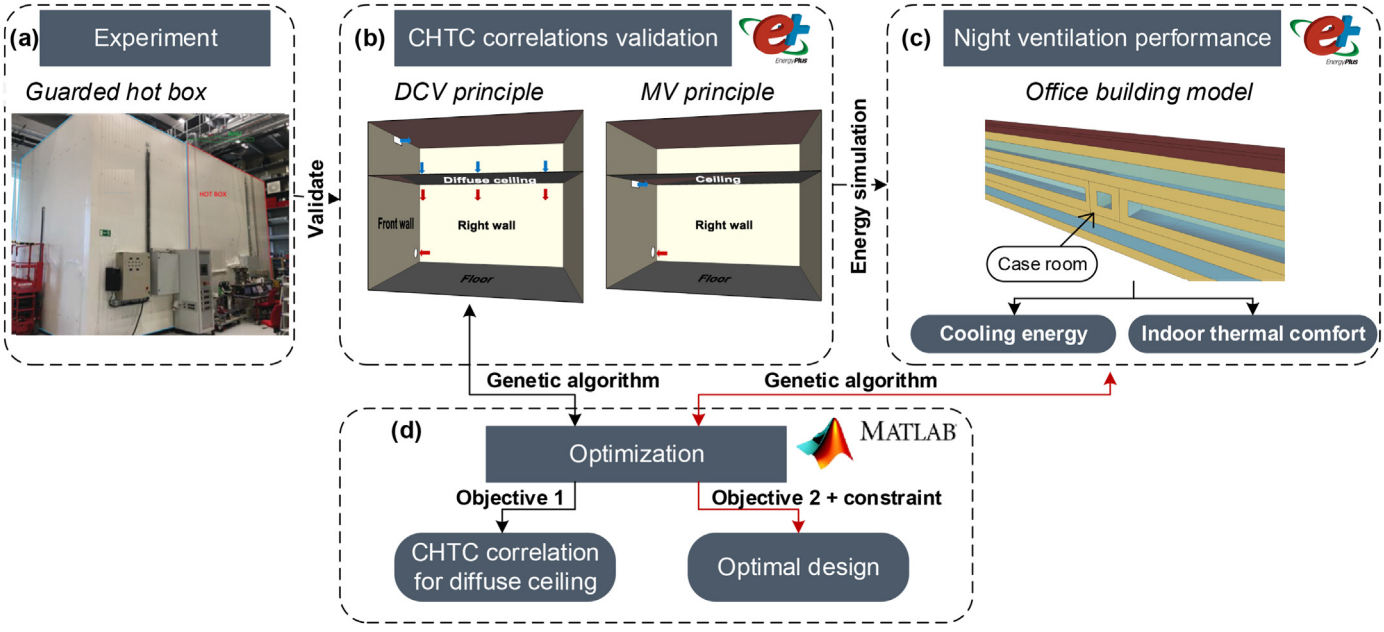

Fig. 1. Flow chart of the proposed research framework.

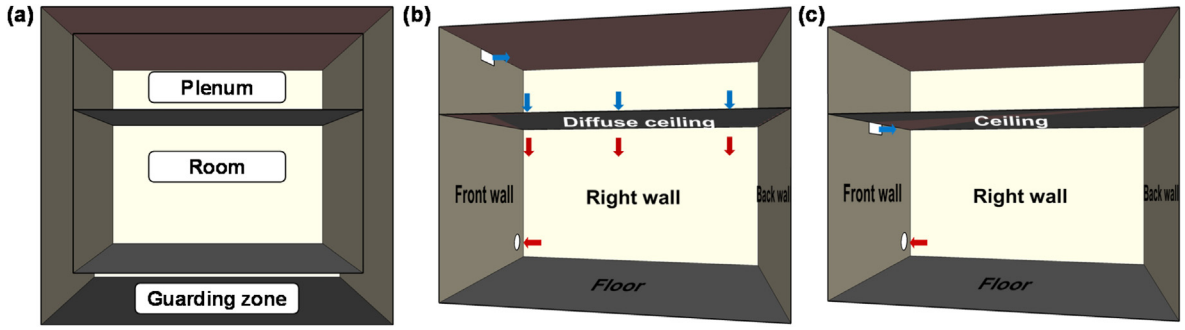

Fig. 2. (a) The guarded hot box model, (b) DCV principle, and (c) MV principle.

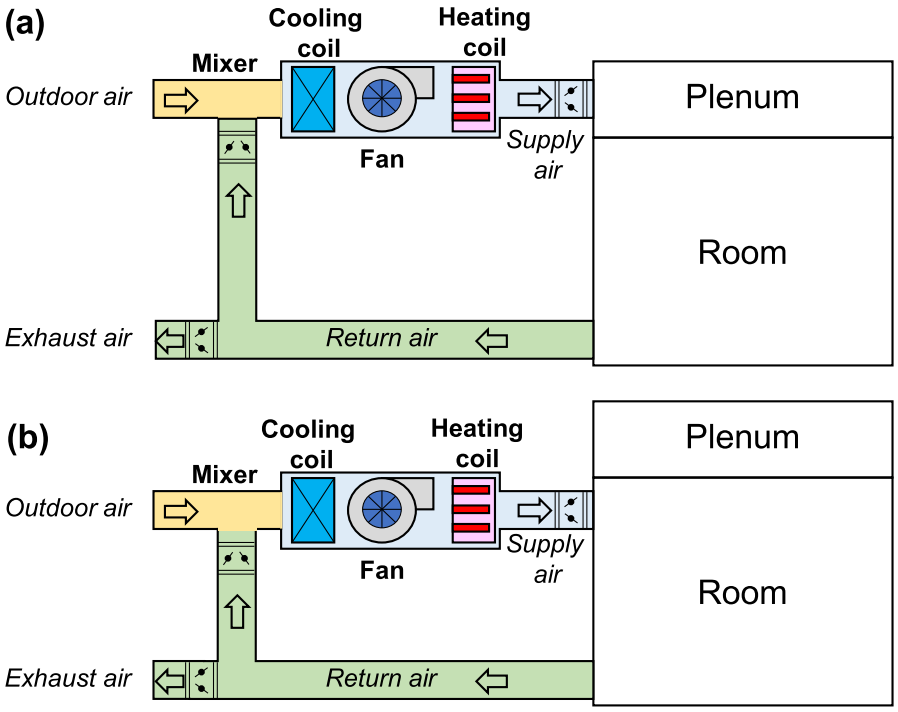

Fig. 3. VAV AC systems for the (a) DCV principle and (b) MV principle.

correlations for the plenum and diffuse ceiling required to be identified and developed as the plenum air temperature was the supply temperature for the room and the diffuse ceiling temperature influenced the radiative heat transfer.

The existing four convection algorithms in EnergyPlus: simple [41], TARP (Thermal Analysis Research Program) [41], ceiling diffuser [42], and adaptive [43], were adopted in turn to identify the most suitable one that provided the minimum MAE between the measured and simulated plenum air temperatures. Each convection algorithm involves various CHTC correlations for the respective interior surfaces of a thermal zone. It is worth noting that the adaptive algorithm is a dynamic algorithm that organizes a large number of different CHTC correlations and automatically selectes the one that best applies for the thermal zone [43]. Six experimental design cases (cf. Table B6 in Appendix B) that included all ranges of supply airflow rates and supply temperatures in the DCV experiment were selected for the correlation identification.

EnergyPlus treats the air exchange and interchange between zones as the convective heat gain rather than modeling the heat transfer through the interface between two zones in detail [8]. Thus, the existing empirical correlations in EnergyPlus were not applicable for the diffuse ceiling. We assume the general form of the forced convection pattern (see Eq. (2)) for the interior surfaces under DCV [32] is also applicable for the diffuse ceiling.

$$h = C_1 + C_2 . ACH^m,\ 0.5 \le m \le 0.8 \tag{2}$$

where h is the CHTC, C_1 and C_2 are constants, and m is an exponent. The optimization method with the genetic algorithm was adopted to develop the diffuse ceiling CHTC correlation, which was further described in Appendix A. The six representative design cases mentioned above were also selected for the correlation development. The optimization objective was to minimize the sum of MAE between the measured and simulated diffuse ceiling temperature of selected design cases (see Eq. (3)). k refers to the index of selected design cases.

$$\min \sum_{k=1}^{6} MAE_k \tag{3}$$

For optimization, C_1 and C_2 were both in the range of (-inf, +inf), and m was in the range of [0.5–0.8]. The population size was set to 50, and the maximum number of generations was set to 200 for the genetic algorithm [44].

3.2. CHTC correlations for plenum and diffuse ceiling under DCV

Table 1 lists the MAE between measured and simulated plenum air temperatures under different convection algorithms. It can be seen that the ceiling diffuser convection algorithm provides the minimum MAE, which ranges between 0.1 °C and 0.4 °C. The average MAE is 0.3 °C. In contrast, the adaptive convection algorithm offers the maximum MAE, indicating that this algorithm cannot automatically select the suitable CHTC correlations for the corresponding surfaces in the plenum.

Table 2 lists the developed diffuse ceiling (facing the room) correlations and the MAE between measured and simulated diffuser ceiling temperatures that ranges between 0.5 °C and 1.3 °C. The mean MAE is 0.6 °C, indicating that the developed correlation can accurately predict the diffuse ceiling surface temperature. Fig. 4 shows the measured and simulated temperatures under the identified ceiling diffuser algorithm and the developed diffuse ceiling correlation. The "m" and "s" in the brackets represent the measured and simulated results. Fig. 4 shows good agreement between the measured and simulated results.

3.3. Validation results of proposed CHTC correlations

Fig. 5 shows the boxplot of the MAE between measured and simulated surface temperatures for different cases. The MAE ranges between 0.1 °C and 1.5 °C for the surface temperatures under DCV, while the MAE ranges between 0.1 °C and 1.9 °C under MV. The median value of MAE for the interior surface temperatures and table surface temperatures under DCV is 0.5 °C and 0.6 °C, respectively. In comparison, the median value of MAE for the interior surface temperatures and table surface temperatures under MV is 0.8 °C and 1.4 °C, respectively. The MAE for table surface temperatures is higher than that for interior surface temperatures. The correlations can be regarded as appropriate for predicting surface temperatures.

The discrepancy between the measured and simulated temperatures can be due to the following reasons: (1) It took some time for the AC to regulate the supply temperature from 22 °C to the specified temperature in the experiment, while the supply temperature in the simulation can reach the temperature setpoint instantaneously. (2) The proposed CHTC correlations were derived from the experimental results that excluded the first hourly data due to the high uncertainties at the beginning of the experiments, which might not take into account the transient flow development at the beginning of night cooling. (3) The uncertainties of measured temperatures and the errors between the experimental CHTCs and predicted CHTCs by the proposed correlations (4) EnergyPlus treated the indoor tables (i.e., internal mass). as virtual horizontal, upward-facing surfaces, resulting in the view factors and radiative heat transfer between table surfaces and interior surfaces being different from the actual values.

Table 1
MAE of measured and simulated plenum air temperature with different convection algorithms.

Convection algorithm	Case 1	Case 2	Case 3	Case 4	Case 5	Case 6
Simple	0.1 °C	0.2 °C	0.3 °C	0.2 °C	0.6 °C	0.1 °C
TARP	0.2 °C	0.1 °C	0.5 °C	0.5 °C	1.1 °C	0.4 °C
Ceiling diffuser	0.4 °C	0.3 °C	0.3 °C	0.1 °C	0.2 °C	0.2 °C
Adaptive	0.3 °C	0.1 °C	0.7 °C	0.6 °C	1.3 °C	0.5 °C

Table 2
MAE of measured and simulated diffuse ceiling temperature with the developed diffuse ceiling CHTC correlation.

CHTC correlation	Case 1	Case 2	Case 3	Case 4	Case 5	Case 6
$-2.23ACH^{0.75}+2.37$	0.3 °C	0.2 °C	0.8 °C	0.6 °C	1.3 °C	0.5 °C

4. Simulation of night ventilation performance

4.1. Case room model

A typical office room, zone 1NC, located on an office building's middle floor [5], was selected as the case room (see Fig. 6). The previous hot box model that excluded the guarding zone was set on zone 1NC, of which the exterior wall facing north was regarded as the "front wall" (see Fig. 2). The boundary conditions for the internal partitions between zone 1NC and the adjacent zones were set as adiabatic by assuming that all adjacent zones have similar thermal conditions. Moreover, an energy-efficient window with a double pane construction made of 3 mm glass and a 13 mm gap filled with argon was located on the exterior wall. The window area was 1.44 m^2, with a total thermal transmittance of 1.06 $W/m^2 \cdot K$, glass solar heat gain coefficient of 0.58, and visible transmittance of 0.70. Two occupants with a load of 126 W/person and the clothing insulation of 0.50 clo were set in zone 1 NC [45,46]. The lighting and electrical appliance were set as 8 W/m^2 and 10 W/m^2, respectively [5]. The hourly schedules for the internal heat gains were 1.0 during the working hours (08:00–17:00) on weekdays and 0 for the remaining periods. The typical meteorological year (TMY3) data [47] of Copenhagen 061800 (IWEC) in summer (July 1 to September 1) was used as the weather inputs.

The VAV AC system introduced in Section 3.1 was also equipped for the case room. The AC operated during the working hours with a cooling setpoint of 24.5 °C and an outdoor airflow of 30 $m^3/(h.person)$ [45]. It should be noticed that the typical supply ACH by HVAC systems to an occupied room ranges from 4 to 6 h^{-1} [2], corresponding to the mean air velocity in the occupied zone of about 0.08 m/s for DCV [48] and 0.2 m/s for MV [49]. The VAV fan also served as the night mechanical ventilation system operated from 17:00 to 08:00 on weekdays. Table 3 shows the specification of the VAV fan and a general NV scheme [2]. The design specific fan power of the fan is 0.86 $kW/(m^3/s)$, which fulfills the recommended 'good-practice' specific fan power for NV [50]. The night ventilation mode pressure rise was lower than the design pressure rise since air can pass through the bypass without flowing through the coils into the room, which was not shown in Fig. 3. The ACH setpoint of the general NV scheme for the room was 10 h^{-1} [2], which equaled the fan's maximum design flow rate. The part-load specific fan power of the VAV fan can be estimated as a function of the fraction of maximum flow rate (r) using Eq. (4). Fig. 7 illustrates the VAV fan performance curve (a = 0.3507, b = 0.3085, c = −0.5413, d = 0.8719) and other performance curves defined in the technical note AIVC 65 [50]. It can be seen that the VAV fan's performance curve falls in between the curves of good and normal systems.

$$\frac{SFP_{part\ load}}{SFP_{max\ load}} \approx a + br + cr^2 + dr^3 \ (0.2 \le r \le 1.0) \quad (4)$$

To compare the performance of night cooling with DCV and MV, the same thermal mass distribution schemes should be both adopted for DCV and MV. Therefore, the 'Not installed', 'Floor', 'Floor + Table' schemes were selected, which represents that the thermal mass (i.e., fiber plasterboards) was not installed in the room, thermal mass was only installed on the floor, and thermal mass was installed on the floor as well as four indoor tables were placed in the room, respectively. The validated correlations in Section 3 were set during the night cooling period. In comparison,

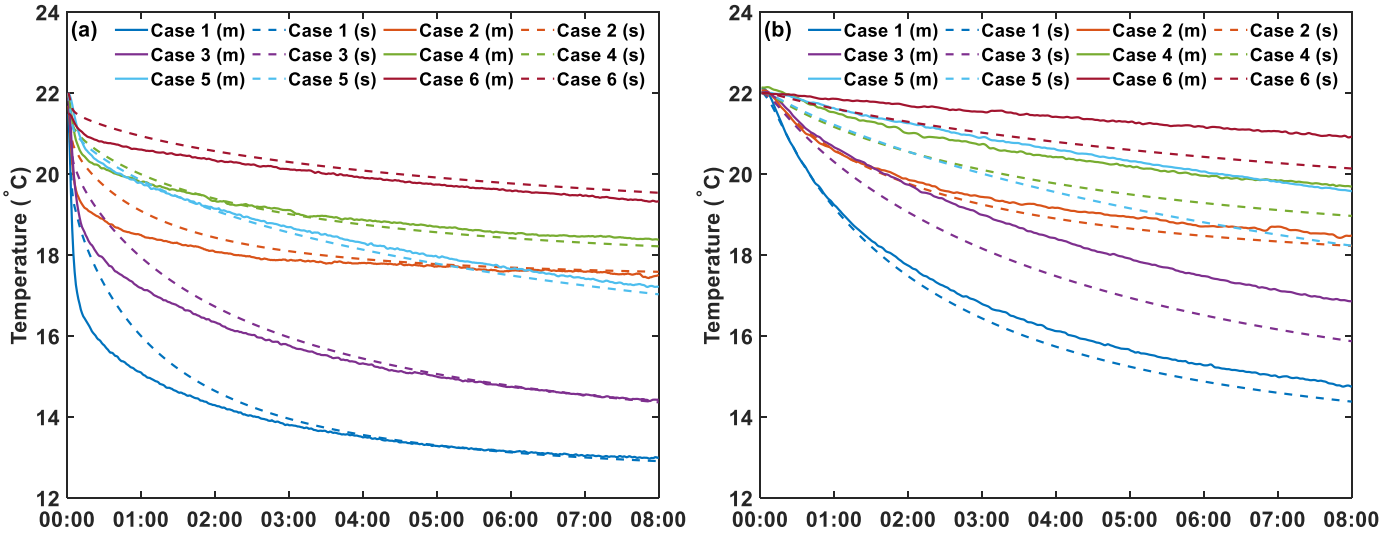

Fig. 4. Comparison of measured and simulated (a) plenum air temperature and (b) diffuse ceiling temperature of selected cases.

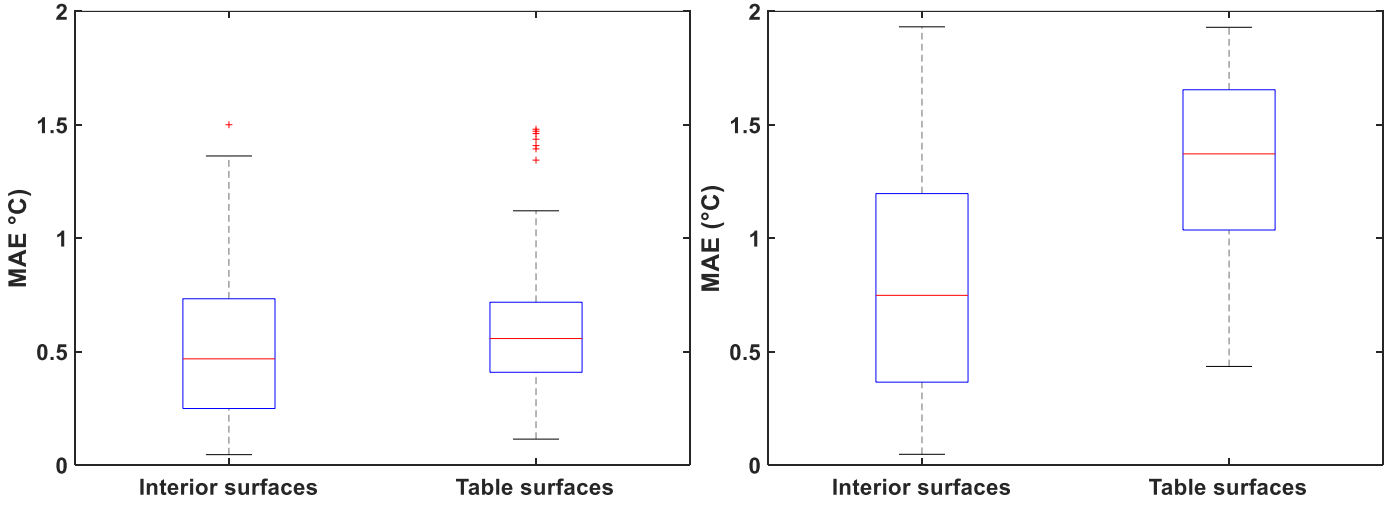

Fig. 5. MAE between measured and simulated temperatures of interior surfaces and table surfaces with proposed CHTC correlations under (a) DCV and (b) MV.

the ceiling diffuser convection algorithm was also set for the room at night. For the two types of simulation cases, the ceiling diffuser convection algorithm was set for the room when the AC operated to eliminate the influence of various correlations on the daytime cooling demand. It is worth noting that for the simulation cases with the validated correlations during the daytime (supply temperature as reference), the ceiling diffuse convection algorithm was the original version [42] (supply temperature as reference) since the EnergyPlus cannot alter the reference temperature during the simulation. While for the simulation cases with the ceiling diffuser convection algorithm all day, the reformulated version (indoor/outlet temperature as reference) [8,51] was adopted since the reformulated algorithm was one of the algorithms built into the EnergyPlus. Because prior experiments did not investigate the CHTC correlation for the window, the existing window correlation under the ceiling diffuser configuration [52] was chosen for the window in the front wall of zone 1NC.

The total (i.e., daytime AC + NV) cooling energy consumption per unit floor area (TCEC) and average predicted percentage of dissatisfied during the working hours (aPPD) were selected as the simulation outputs to evaluate the NV performance.

4.2. Performance of night cooling with DCV and MV

Fig. 8 shows the simulated results of MV cases. When the room was only cooled with the AC, the MV cases with two versions of ceiling diffuser convection algorithm under the same thermal mass distribution had similar energy use and indoor thermal comfort level. The discrepancy can be attributed to the different reference temperatures of reformulated and original convection algorithms during the daytime.

Compared to the respective MV cases without night cooling in Fig. 8a, NV saved the TCEC by 0.6 kWh/m^2 (17.1%) – 1.0 kWh/m^2 (26.0%) but increased the aPPD by 2.6%–9.4%. Whereas for corresponding MV cases in Fig. 8b, NV reduced the TCEC by 0.3 kWh/m^2 (8.6%) – 0.5 kWh/m^2 (13.8%) but increased the aPPD by 2.4%–6.4%. It can be concluded that the ceiling diffuser algorithm overestimated the night energy-saving potential by 0.3 kWh/m^2 (8.6%) – 0.5 kWh/m^2 (13.8%) and yielded a difference in aPPD between −0.9% and 1.5%, compared to the validated correlations for MV. The reason causes the performance discrepancy should be that the validated CHTC correlations induced a smaller night airflow rate than the ceiling diffuser algorithm.

Fig. 8 also shows that the aPPD of most night-cooled cases was

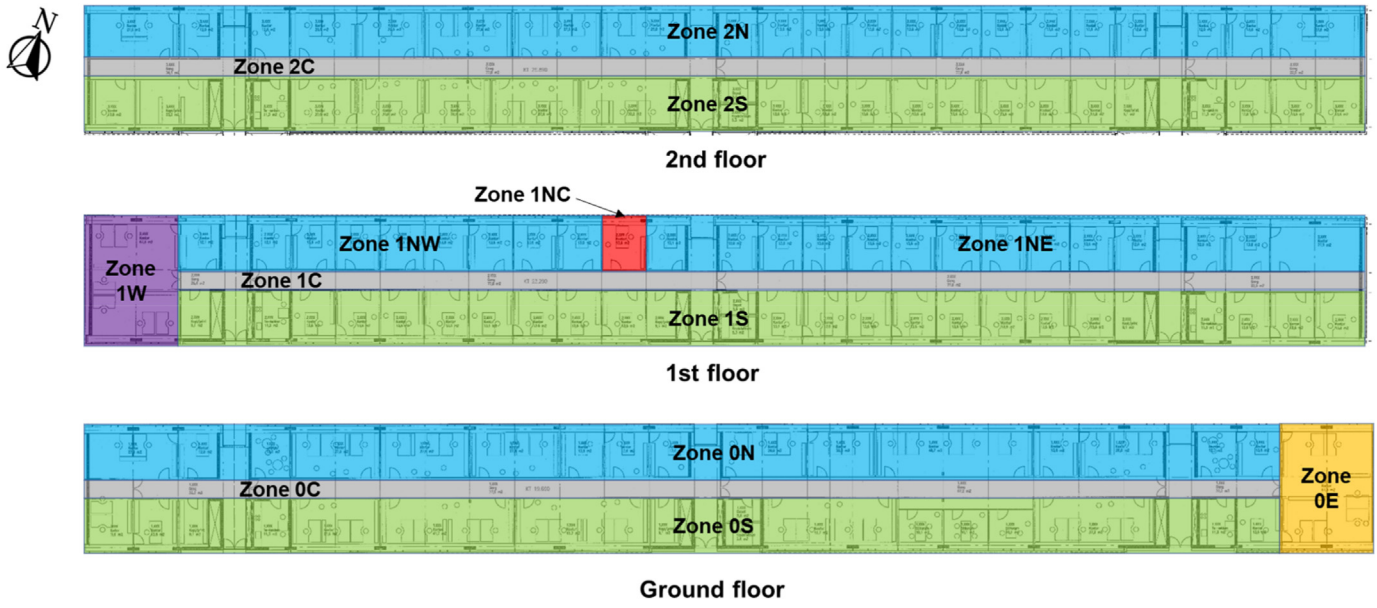

Fig. 6. Layout of the case building and the case room 1NC.

Table 3
Detailed setup information about the night mechanical ventilation system.

Night mechanical ventilation	
System	VAV supply fan
Design pressure rise (Pa)	600
Fan total efficiency	0.7
Specific fan power (kW/(m^3/s))	0.86
Maximum design flow rate (m^3/s)	0.0972
Night ventilation mode pressure rise (Pa)	67
Minimum indoor temperature setpoint (°C)	18
Activation threshold temperature (°C)	3

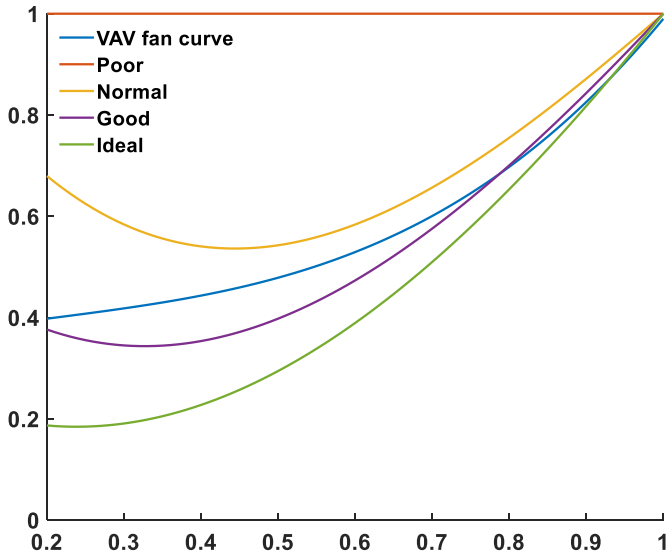

Fig. 7. Illustration of performance curves of the VAV fan, poor, normal, good, and ideal systems [50].

over 10% that was the recommended PPD of category II for mechanically cooled buildings [45]. Fig. 9 shows the simulated hourly indoor air, ceiling, and floor (on behalf of all the interior surfaces) temperatures of an MV case ('Floor + Table(b)') with and without night cooling in Fig. 8a on a typical summer day. On the selected night, the NV significantly reduced the indoor temperatures up to 8.5 °C. At the beginning of working hours, the indoor temperatures were all about 20.5 °C, which postponed AC's operation until 12:00 but made the occupants feel cold.

Furthermore, by comparing the night-cooled MV cases, it was found that NV saved the most energy but provided the highest aPPD for the case with the highest thermal mass level. On the contrary, the MV case with the low thermal mass level had the smallest night cooling energy saving potential and the lowest aPPD. One reason was that high thermal mass could stabilize the indoor air temperature and store more excess heat instead of being removed by the AC during the daytime. The stored excess heat can then be released and removed by night cooling. Another reason was that the interior surface with thermal mass had higher thermal inertia and a larger CHTC, whose temperature grew slowly when NV was adopted. Fig. 9 also shows that the night-cooled floor (with thermal mass) temperature was approximately 1 °C lower than the indoor and ceiling temperature at the beginning of working hours. Moreover, by comparing the MV cases with tables in Fig. 8b, it was found that the position of tables had a neglectable effect on the performance of night cooling with MV.

Fig. 10 shows the simulated results of DCV. Since the proposed correlations for indoor tables did not distinguish the tables' position, the simulation case for DCV with tables was only one. For the cases shown in Fig. 10a, NV saved the TCEC by 0.8 kWh/m^2 (21.0%) – 1.2 kWh/m^2 (30.8%) but rose the aPPD by 1.7%–6.4%, compared to the respective cases without NV. Whereas in Fig. 10b, NV cut the TCEC by 0.5 kWh/m^2 (13.2%) – 0.7 kWh/m^2 (18.0%), while the aPPD increased by 1.7%–3.8%. The ceiling diffuser algorithm overestimated the night energy-saving potential by 0.3 kWh/m^2 (7.8%) – 0.5 kWh/m^2 (12.8%) and yielded a difference in aPPD between −0.9% – 1.3%, compared to the validated CHTC correlations for DCV.

Furthermore, by comparing the cases in Figs. 8b and 10b, DCV consumed about 0.3 kWh/m^2 more TCEC than MV for the conditioned room without NV since the AC took the internal heat load in the plenum under DCV. On the contrary, night cooling with DCV

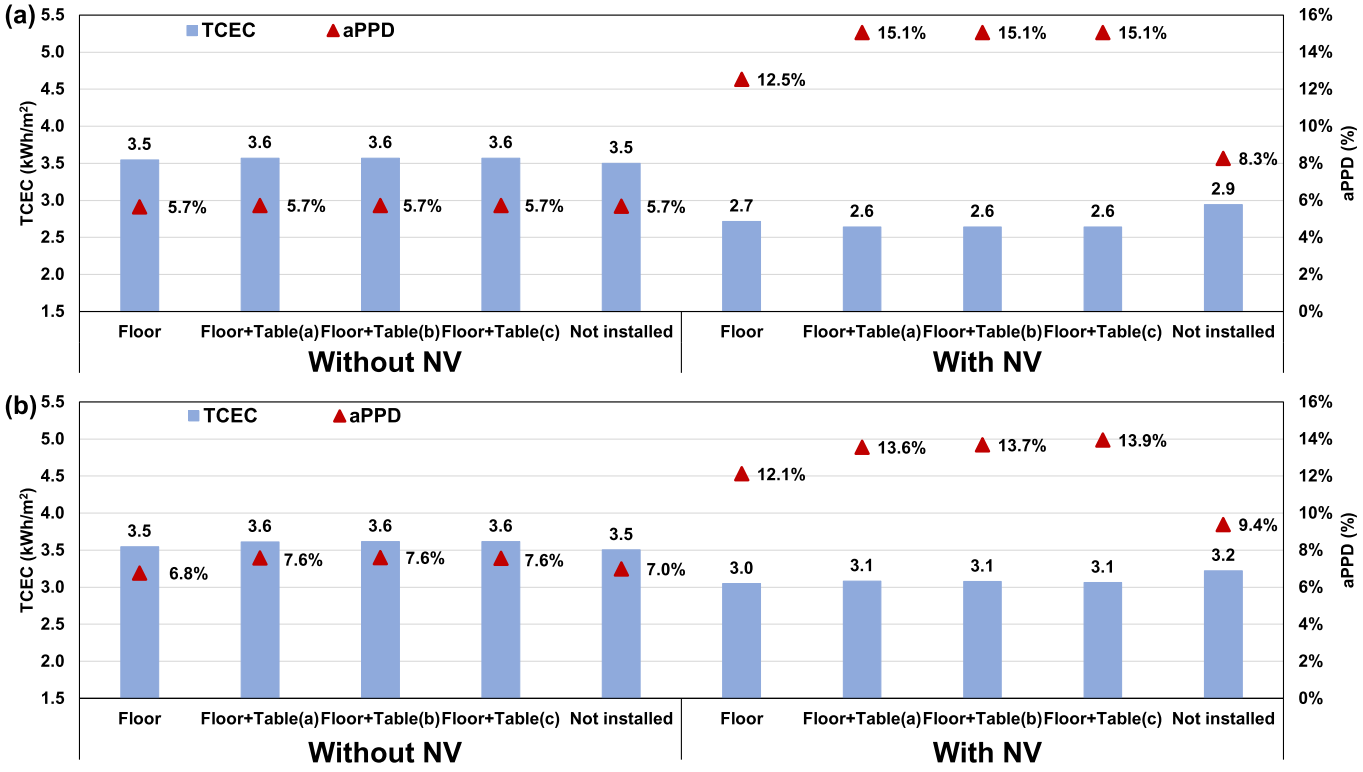

Fig. 8. Simulated TCEC and aPPD of MV cases with (a) ceiling diffuser convection algorithm and (b) validated CHTC correlations at night.

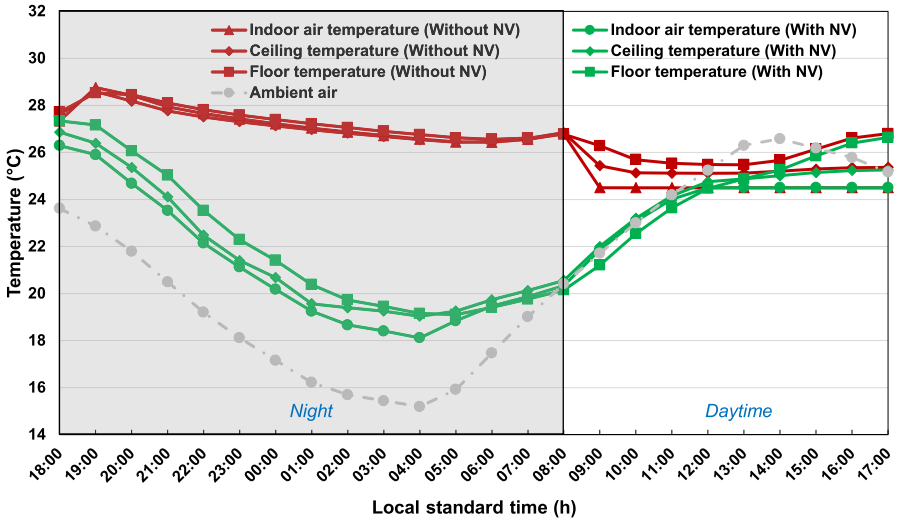

Fig. 9. Simulated indoor air, ceiling, and floor temperatures of the selected MV case with and without NV on a typical summer day (August 1 to August 2).

saved about 0.2 kWh/m^2 TCEC more than that with MV. The reason was that the plenum was also cooled down by the cold outdoor air at night, which can be a heat sink during the daytime. Apart from the energy performance, night cooling with DCV contributed to a lower aPPD of 0.9%–3.1% compared to MV. The reasons were twofold: (1) The air velocity in the occupied zone under DCV (0.08 m/s) was smaller than the velocity (0.2 m/s) under MV. (2) Night cooling with DCV cooled down both the plenum and the room, resulting in relatively high indoor temperatures and a small overcooling penalty, compared to the same case with MV.

5. Optimal design of night ventilation

5.1. Optimization setup

Simulation results of night cooling performance in Section 4 indicated that the general NV scheme can save the cooling energy use but may also cause the overcooling penalty to make occupants feel cold. Optimization provides a way to improve energy-saving potential while maintaining indoor thermal comfort within a certain level [53]. The recommended category II of PPD (<10%) in EN 15251 [45] for designing the buildings with mechanical cooling

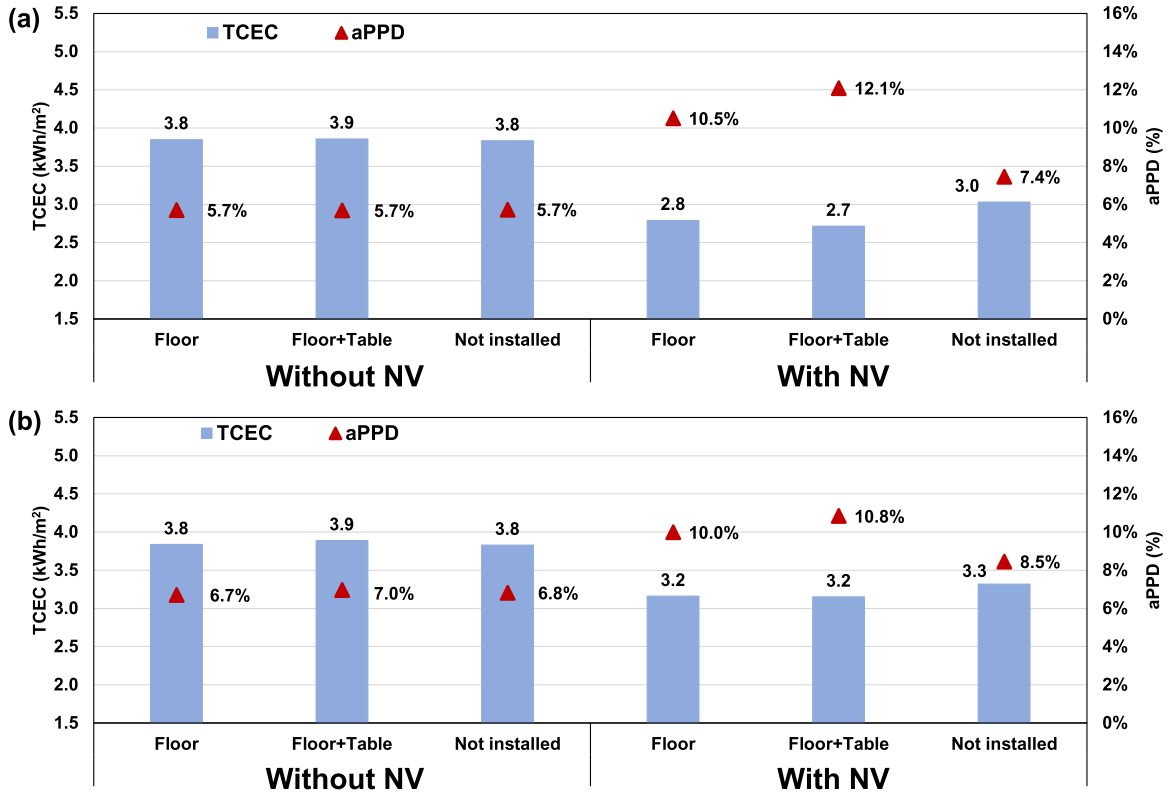

Fig. 10. Simulated TCEC and aPPD of DCV cases with (a) ceiling diffuser convection algorithm and (b) validated CHTC correlations at night.

was selected as the constraint for indoor thermal comfort. Therefore, the optimization problem can be formulated as a single objective with a single constraint problem expressed by Eqs. (5) and (6)

$$\min \ TCEC \tag{5}$$

$$\text{subject to } aPPD < 10\% \tag{6}$$

The genetic algorithm was also adopted by coupling the EnergyPlus with MATLAB (see Appendix A). The population size for the genetic algorithm was set to 200, and the maximum generations were set to 200 [44,54]. The DCV and MV cases without thermal mass distribution (i.e., 'Not installed') were selected as the base cases.

Table 4 summarizes the parameters to be optimized. O1 provided the flexibility to investigate the optimal night cooling airflow and duration [40]. The hourly ACH setpoint did not range between 0 and 0.2 as the minimum fraction (i.e., r in Eq. (4)) of maximum flow rate for the VAV fan was 0.2. O2 and O3 had an interactive effect on the energy use and thermal comfort. Increasing the value of O2 can reduce the risk of the overcooling penalty but decreased the utilization of night cooling, requiring the value of O3 to be lower to maintain the indoor thermal comfort and use more cooling energy, vice versa. The range of O3 originated from the maximum temperature range for the cooling setpoint in summer [45]. In contrast, the range of O2 was from the minimum cooling setpoint in Ref. [45] and the lowest setpoint in Ref. [9]. A step of 0.5 °C was set for the O2 and O3 due to the general precision of temperature measurement and control precision for HVAC systems. Based on the validated proposed CHTC correlations, four thermal mass distribution schemes for DCV were 'Not installed', 'Floor', 'Table', 'Floor + Table'. Because the indoor tables' position had a limited influence on the cooling energy use and indoor thermal comfort under MV, only the position of 'Table(c)' was selected due to the relatively low TCEC and aPPD. Therefore, the candidate schemes for MV can be the combination of the ceiling with thermal mass or not, floor with thermal mass or not, right wall with thermal mass or not, with indoor tables or not. Thanks to the EP-Macro program of EnergyPlus [55], O4 can be set separately from the base cases and inserted in the base cases during the optimization.

5.2. Optimal design solutions

Fig. 11 shows the parameters of the optimal cases as well as the base cases with the general NV scheme. Both the optimal DCV and MV cases were equipped with their maximum investigated thermal mass level and had the maximum allowed AC cooling temperature setpoint (i.e., 27 °C). This can be explained that a higher AC temperature setpoint can reduce the cooling energy use during the daytime and leave more excess heat stored in the high thermal mass level, which can be removed by night cooling without causing the overcooling penalty. In comparison with the optimal MV case, the optimal DCV case had a lower minimum indoor air temperature setpoint (i.e., 16 °C) for NV. It indicated that DCV allowed a larger night cooling potential due to the excess heat stored in the plenum were removed at night and the low air velocity in the occupied zone during the daytime. The hourly night ACH setpoints of the two optimal cases varied significantly and were both smaller than the general NV scheme (i.e., 10 h^{-1}). A general trend was that the hourly ACH setpoints were high in the first half of the night to cool down the building effectively and then decreased before the next working hours to reduce the risk of overcooling penalty.

Fig. 12 shows the simulated results of the research cases. Compared with the respective base cases (i.e., without thermal mass and NV), the optimal DCV and MV case significantly saved the TCEC by 1.1 kWh/m^2 (29.0%) and 0.9 kWh/m^2 (25.7%), respectively,

Table 4
Range and distribution of parameters for optimization.

Parameter		Unit	Range
O1	NV hourly ACH setpoint	h^{-1}	0 or **D** [2–10] with a step of 0.1 h^{-1} at each hour of per weekday night
O2	Minimum indoor temperature setpoint	°C	**D** [16–22] with a step of 0.5 °C
O3	AC temperature setpoint	°C	**D** [22–27] with a step of 0.5 °C
O4	Thermal mass distribution schemes	-	4 schemes for DCV and 16 schemes for MV

Note: **D**: discrete distribution (levels).

while maintaining the aPPD within the prescribed limit (i.e., 10%). The performance of DCV improved more after the optimization, especially the investigated highest thermal mass level for DCV was smaller than that for MV.

Additionally, the base cases with the general NV scheme were also simulated to demonstrate the optimization effect. The night-cooled base cases also saved the cooling energy, increased the aPPD, and the aPPD remained below 10%. In contrast, the optimal cases can further save energy by 0.6 kWh/m^2 (18.2%) for DCV and 0.6 kWh/m^2 (18.6%) for MV, respectively, without violating the thermal comfort requirement. When the DCV case and MV case were equipped with respective maximum thermal mass levels (i.e., same as their optimal cases) and the general NV scheme, the cooling energy further reduced, but the aPPD exceeded the 10% up to 17.1%, compared with respective night-cooled base cases. After optimizing those cases, the optimal cases saved the TCEC by 0.5 kWh/m^2 (15.6%) for DCV and 0.3 kWh/m^2 (10.4%) for MV and significantly reduced the aPPD.

6. Conclusions and future work

This study presents a holistic approach to validate the experimentally proposed convective heat transfer (CHTC) correlations for night cooling with diffuse ceiling ventilation (DCV) and mixing ventilation (MV), simulate, and optimize the performance of night cooling with DCV and MV. Based on the results of the case study, the following conclusions can be made.

- For DCV, the empirical ceiling diffuser convection algorithm was able to predict the plenum air temperature accurately. Furthermore, the correlation for the suspended ceiling panel was developed to precisely predict the ceiling temperature. Finally, the proposed correlations for MV and DCV were applicable to predict the interior surface temperature accurately.
- DCV consumed about 0.3 kWh/m^2 total cooling energy consumption per floor area (TCEC) more than MV for the conditioned room. However, a general night cooling scheme with DCV offers a larger energy-saving potential and better indoor thermal comfort, saving about 0.2 kWh/m^2 TCEC more and contributing to the average predicted percentage of dissatisfied during the working hours (aPPD) as low as 3.1% than that with MV.
- The empirical ceiling diffuser convection algorithm overestimated the night energy-saving potential up to 0.5 kWh/m^2 (13.8%) TCEC and yielded a difference in a PPD up to 1.5%, compared to the validated correlations for DCV and MV.
- Optimization for MV and DCV tends to equip the room with the higher thermal mass level and daytime air conditioning cooling setpoint but the lower minimum indoor air temperature setpoint and hourly night air change rate setpoint. Compared with the respective base cases, the optimal DCV and MV case can significantly save TCEC by 1.1 kWh/m^2 (29.0%) and 0.9 kWh/m^2 (25.7%), respectively, while maintaining indoor thermal comfort. The performance of night cooling with DCV improved more after the optimization.

It is worth noting that the validated CHTC correlations can also be leveraged to investigate the performance of all-day mechanical ventilation with DCV and MV. The investigated correlations for the plenum and diffuse ceiling provide the potential to study the annual energy and thermal performance of the DCV principle, where few studies focused on this area. The optimization method allows architects or engineers to improve the night cooling performance at the building level, with different climate conditions, cooling systems, and thermal comfort requirements.

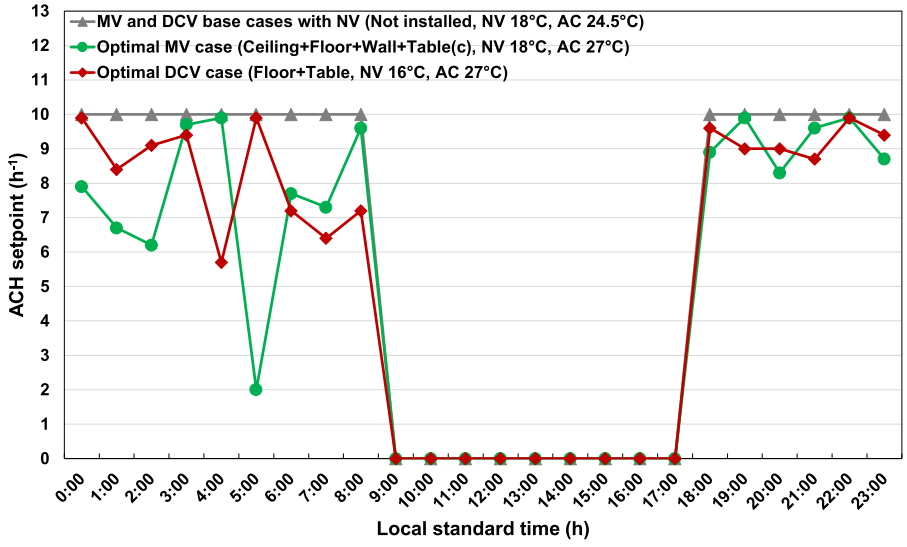

Fig. 11. Parameters related to cooling systems of the research cases.

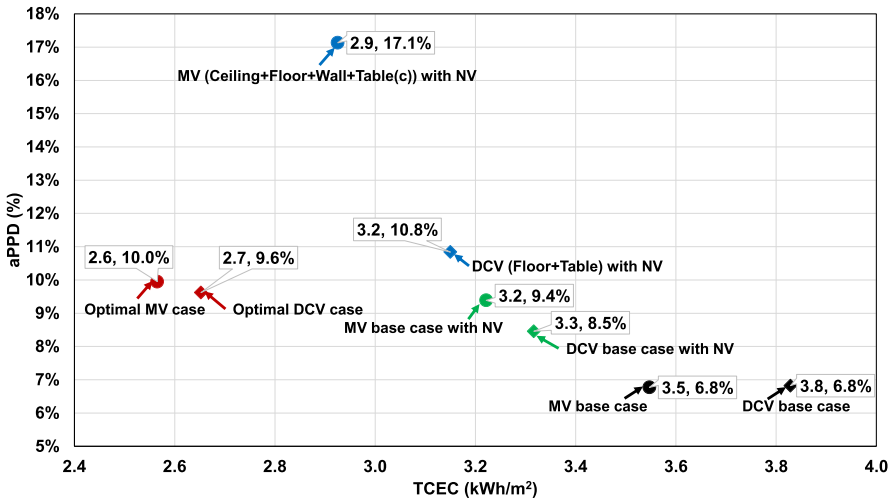

Fig. 12. Simulated TECE and aPPD of the research cases.

Since the CHTC correlations with the supply reference temperature are only available for the mechanical cooling system in the latest version of EnergyPlus, which limits the application of those validated correlations in the natural ventilation system. Moreover, the optimal solutions are based on the TMY3 data. Therefore, future climate change should be taken into account to make the optimal solutions more resilient.

CRediT authorship contribution statement

Rui Guo: Conceptualization, Data curation, Methodology, Writing – review & editing. **Yue Hu:** Investigation, Visualization, Writing – review & editing. **Per Heiselberg:** Supervision, Project administration, Writing – review & editing. **Hicham Johra:** Visualization, Writing – review & editing. **Chen Zhang:** Visualization, Writing – review & editing. **Pei Peng:** Visualization, Writing – review & editing.

Declaration of competing interest

The authors declare that they have no known competing financial interests or personal relationships that could have appeared to influence the work reported in this paper.

Acknowledgments

The project is carried out as part of IEA EBC Annex 80 Resilient Cooling. The first author gratefully acknowledges the financial support from the China Scholarship Council (CSC No. 201706050001).

Appendix A. Optimization framework

Fig. A1 shows the proposed optimization framework in this study. The first step was to construct the model. The Input Data File (IDF) files contained the model information in EnergyPlus and were simulated to offer the results to comma-separated value (CSV) text files. The second step was to build a coupling engine in MATLAB that loaded the IDF files as the data structure in MATLAB and tuned the parameters in the IDF files based on the decision variables of the optimization problem in each iteration. The modified IDF files were then sent back to EnergyPlus for simulation to return the simulation results evaluated by the objective functions and or constraints. To speed up the optimization, the Parallel Computing Toolbox™ [56] in MATLAB was used to distribute tasks parallelly rather than distributing tasks serially. In the third step, one optimization algorithm of the Global Optimization Toolbox™ [44] in MATLAB, genetic algorithm, was leveraged to obtain the optimal solutions. The process was repeated until the genetic algorithm converged to offer the optimal solution for the optimization problem [57].

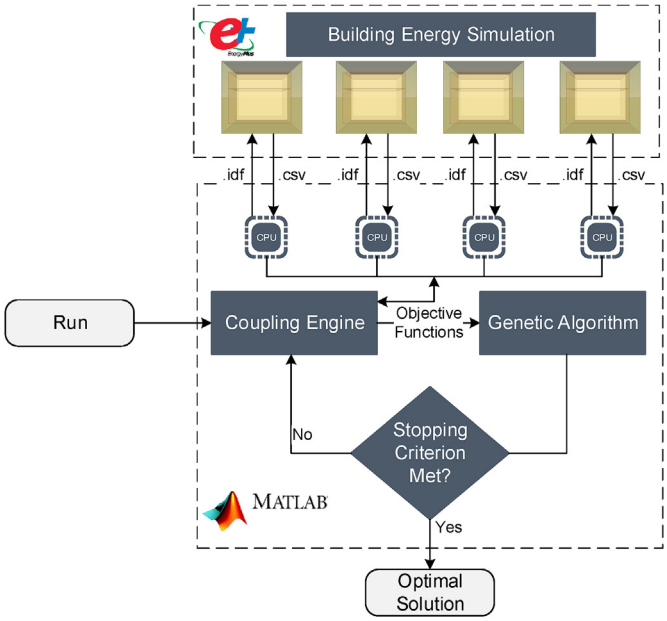

Fig. A1. Proposed optimization framework.

Appendix B. Experimental description

Table B1 shows the main features of the guarded hot box [32,33]. There were 25 design cases for the DCV experiment and 48 design cases for the MV experiment. Those design cases differed in supply ACH, supply temperatures, and thermal mass (i.e., fiber plasterboards) distribution schemes. For each design case, an air handling unit continuously supplied the conditioned at the specified airflow rate and air temperature to the unoccupied room for 8 h to simulate the night cooling. Another air handling unit supplied the conditioned air to the guarding zone for a stable outdoor

environment by maintaining the zone air temperature at 22 °C. The 18 mm fiber plasterboards (ρ = 1150 kg/m^3, C_p = 1100 J/kg·K, λ = 0.32 W/m·K) were installed on other room's interior surfaces for different design cases. Besides, some design cases had the furniture (i.e., four indoor tables), of which each table was made up of two fiber plasterboards. The thickness and area of each table was 36 mm and 1.08 m^2, respectively. Fig. B1 shows the positions of indoor tables.

same nonlinear least square method as in Refs. [32,33]. The difference was that the proposed correlations in this study were only based on the criteria of one surface had thermal mass or not rather than taking into account the conditions of other surfaces. They will provide high flexibility to investigate more thermal mass distribution schemes than the experimentally investigated schemes. It is worth noting that the correlation for the diffuse ceiling was not developed in the DCV experiment due to the complex heat transfer

Table B1Main features of the guarded hot box.

Dimensions	
Plenum	4.2 m (L) × 3.6 m (W) × 2.5 m (H)
Room	4.2 m (L) × 3.6 m (W) × 1.1 m (H)
Guarding zone	5.1 m (L) × 4.6 m (W) × 4.6 m (H)
Original envelope of the room	
Front wall	Three layers (outside to inside: 150 mm foam boards, 12 mm wood panel, and 100 mm foam boards) with total thermal transmittance of 0.15 W/m^2·K
Right wall, left wall, and floor	Four layers (outside to inside: 15 mm wood panel, 225 mm expanded polystyrene, 15 mm wood panel, and 50 mm foam boards) with total thermal transmittance of 0.14 W/m^2·K
Back wall	Four layers (outside to inside: 15 mm wood panel, 225 mm expanded polystyrene, 15 mm wood panel, and 100 mm foam boards) with total thermal transmittance of 0.12 W/m^2·K
Ceiling	For DCV: one layer (25 mm wood-cement board with the 65% porosity) with total thermal transmittance of 3.4 W/m^2·K For MV: two layers (outside to inside: 15 mm wood panel and 50 mm foam boards) with total thermal transmittance of 0.68 W/m^2·K
Original envelope of the plenum	
Walls and ceiling	Three layers (outside to inside: 15 mm wood panel, 225 mm expanded polystyrene, 15 mm wood panel) with total thermal transmittance of 0.24 W/m^2·K
Floor	For DCV: one layer (25 mm wood-cement board with the 65% porosity) with total thermal transmittance of 3.4 W/m^2·K For MV: two layers (outside to inside: 50 mm foam boards and 15 mm wood panel) with total thermal transmittance of 0.68 W/m^2·K
Envelope of the guarding zone	
Walls, ceiling, and floor	Three layers (outside to inside: 15 mm wood panel, 225 mm expanded polystyrene, 15 mm wood panel) with total thermal transmittance of 0.24 W/m^2·K

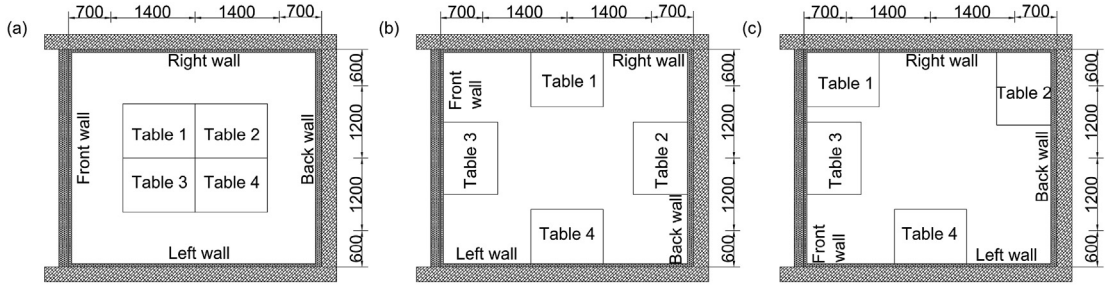

Fig. B1. Positions of indoor tables (a) in the middle, (b) close to walls, and (c) close to the corners or the walls of the room [32,33].

Tables B2 to B5 list the proposed CHTC correlations (with supply reference temperature) for night cooling with DCV and MV. The dash in the Tables indicated that the correlation was not proposed. The correlations for interior surfaces (i.e., Table B2, Table B4) were also developed based on the same experimental CHTCs using the through the porous diffuse ceiling panel, which needed BES for further investigation in Section 3. It is also worth noting that the correlations for tables under MV depended on the location of tables and the table's face orientation, while those correlations for tables under DCV only depended on the table's face orientation.

Table B2
CHTC correlations for interior surfaces under night cooling with DCV [32].

With thermal mass or not	Front wall	Right wall	Back wall	Left wall	Floor
Yes	–	–	–	–	$0.17ACH^{0.8}+0.67$
No	$0.15ACH^{0.5}+0.1$	$0.17ACH^{0.5}-0.11$	$0.08ACH^{0.8}-0.08$	$0.08ACH^{0.8}-0.07$	$0.08ACH^{0.8}+0.11$

Table B3
CHTC correlations for indoor furniture under night cooling with DCV [32].

Table surface	Correlation
Facing upward	$0.19ACH^{0.65}+0.11$
Facing downward	$0.1ACH^{0.65}-0.21$

Table B4
CHTC correlations for interior surfaces under night cooling with MV [33].

With thermal mass or not	Front wall	Right wall	Back wall	Left wall	Floor	Ceiling
Yes	–	$0.12ACH^{0.8}+0.13$	–	–	$0.28ACH^{0.8}+0.36$	$1.07ACH^{0.5}-0.94$
No	$0.1ACH^{0.8}-0.01$	$0.22ACH^{0.8}+0.46$	$0.55ACH^{0.5}-0.41$	$0.08ACH^{0.8}+0.07$	$0.06ACH^{0.8}+0.2$	$0.92ACH^{0.5}-1.17$

Table B5
CHTC correlations for indoor tables under night cooling with MV [33].

Table's Position	Table 1 upward-facing surface	Table 1 downward-facing surface	Table 2 upward-facing surface	Table 2 downward-facing surface	Table 3 upward-facing surface	Table 3 downward-facing surface	Table 4 upward-facing surface	Table 4 downward-facing surface
Table(a)	$0.19ACH^{0.8}-0.5$	$0.16ACH^{0.8}-0.09$	$0.12ACH^{0.8}-0.35$	$0.53ACH^{0.5}-0.46$	$0.14ACH^{0.5}-0.19$	$0.11ACH^{0.8}-0.07$	$0.08ACH^{0.8}-0.13$	$0.12ACH^{0.8}-0.04$
Table(b)	$0.14ACH^{0.8}-0.02$	$0.16ACH^{0.8}-0.2$	$0.16ACH^{0.8}-0.01$	$0.16ACH^{0.7}-0.11$	$0.03ACH^{0.8}-0.02$	$0.31ACH^{0.5}-0.39$	$0.02ACH^{0.8}+0.2$	$0.12ACH^{0.8}-0.06$
Table(c)	$0.12ACH^{0.8}-0.06$	$0.13ACH^{0.8}-0.29$	$0.04ACH^{0.8}-0.25$	$0.59ACH^{0.5}-0.62$	$0.07ACH^{0.8}-0.11$	$0.34ACH^{0.5}-0.46$	$0.01ACH^{0.8}+0.24$	$0.15ACH^{0.8}-0.05$

Table B6
Selected representative design cases in the DCV experiment.

Design case	Thermal mass distribution	ACH (h^{-1})	T_{sup} (°C)
1	Floor	10	12
2	Floor	10	17
3	Floor	5	12
4	Floor	5	17
5	Floor	2	12
6	Floor	2	17

References

[1] M. Kolokotroni, P. Heiselberg, Ventilative Cooling: State-Of-The-Art Review, Aalborg Univ. Aalborg, Denmark, 2015. https://www.buildup.eu/en/node/52462.

[2] A. O'Donnavan, A. Belleri, F. Flourentzou, G.-Q. Zhang, G.C. da Graca, H. Breesch, M. Justo-Alonso, M. Kolokotroni, M.Z. Pomianowski, P. O'Sullivan, Others, Ventilative Cooling Design Guide, Aalborg University, Department of Civil Engineering, 2018. https://venticool.eu/wp-content/uploads/2016/11/VC-Design-Guide-EBC-Annex-62-March-2018.pdf.

[3] N. Artmann, H. Manz, P. Heiselberg, Parameter study on performance of building cooling by night-time ventilation, Renew. Energy 33 (2008) 2589–2598, https://doi.org/10.1016/j.renene.2008.02.025.

[4] X. Xie, O. Sahin, Z. Luo, R. Yao, Impact of neighbourhood-scale climate characteristics on building heating demand and night ventilation cooling potential, Renew. Energy 150 (2020) 943–956, https://doi.org/10.1016/j.renene.2019.11.148.

[5] R. Guo, Y. Hu, M. Liu, P. Heiselberg, Influence of design parameters on the night ventilation performance in office buildings based on sensitivity analysis, Sustain. Cities Soc. 50 (2019) 101661, https://doi.org/10.1016/j.scs.2019.101661.

[6] E. Solgi, Z. Hamedani, R. Fernando, H. Skates, N.E. Orji, A literature review of night ventilation strategies in buildings, Energy Build. 173 (2018) 337–352, https://doi.org/10.1016/j.enbuild.2018.05.052.

[7] L. Peeters, I. Beausoleil-Morrison, A. Novoselac, Internal convective heat transfer modeling: critical review and discussion of experimentally derived correlations, Energy Build. 43 (2011) 2227–2239, https://doi.org/10.1016/j.enbuild.2011.05.002.

[8] U.S. Department of Energy, EnergyPlus 9.3 engineering reference. https://bigladdersoftware.com/epx/docs/9-3/engineering-reference/, 2020.

[9] K. Goethals, H. Breesch, A. Janssens, Sensitivity analysis of predicted night cooling performance to internal convective heat transfer modelling, Energy Build. 43 (2011) 2429–2441, https://doi.org/10.1016/j.enbuild.2011.05.033.

[10] N. Artmann, R.L. Jensen, H. Manz, P. Heiselberg, Experimental investigation of heat transfer during night-time ventilation, Energy Build. 42 (2010) 366–374, https://doi.org/10.1016/j.enbuild.2009.10.003.

[11] J. Le Dréau, P. Heiselberg, R.L. Jensen, Experimental investigation of convective heat transfer during night cooling with different ventilation systems and surface emissivities, Energy Build. 61 (2013) 308–317, https://doi.org/10.1016/j.enbuild.2013.02.021.

[12] W. Ji, Q. Luo, Z. Zhang, H. Wang, T. Du, P.K. Heiselberg, Investigation on thermal performance of the wall-mounted attached ventilation for night cooling under hot summer conditions, Build. Environ. 146 (2018) 268–279, https://doi.org/10.1016/j.buildenv.2018.10.002.

[13] W. Ji, H. Wang, T. Du, Z. Zhang, Parametric study on a wall-mounted attached ventilation system for night cooling with different supply air conditions, Renew. Energy 143 (2019) 1865–1876, https://doi.org/10.1016/j.renene.2019.06.022.

[14] D. Olsthoorn, F. Haghighat, A. Moreau, G. Lacroix, Abilities and limitations of thermal mass activation for thermal comfort, peak shifting and shaving: a review, Build. Environ. 118 (2017) 113–127, https://doi.org/10.1016/J.BUILDENV.2017.03.029.

[15] V. Geros, M. Santamouris, A. Tsangrasoulis, G. Guarracino, Experimental evaluation of night ventilation phenomena, Energy Build. 29 (1999) 141–154, https://doi.org/10.1016/S0378-7788(98)00056-5.

[16] A. Michael, D. Demosthenous, M. Philokyprou, Natural ventilation for cooling in mediterranean climate: a case study in vernacular architecture of Cyprus, Energy Build. 144 (2017) 333–345, https://doi.org/10.1016/j.enbuild.2017.03.040.

[17] S. Leenknegt, R. Wagemakers, W. Bosschaerts, D. Saelens, Numerical study of convection during night cooling and the implications for convection modeling in Building Energy Simulation models, Energy Build. 64 (2013) 41–52, https://doi.org/10.1016/j.enbuild.2013.04.012.

[18] Y. Liu, L. Yang, L. Hou, S. Li, J. Yang, Q. Wang, A porous building approach for modelling flow and heat transfer around and inside an isolated building on night ventilation and thermal mass, Energy 141 (2017) 1914–1927, https://doi.org/10.1016/j.energy.2017.11.137.

[19] J. Liu, Y. Liu, L. Yang, T. Liu, C. Zhang, H. Dong, Climatic and seasonal suitability of phase change materials coupled with night ventilation for office buildings in Western China, Renew. Energy 147 (2019) 356–373, https://doi.org/10.1016/j.renene.2019.08.069.

[20] Y. Hu, P.K. Heiselberg, H. Johra, R. Guo, Experimental and numerical study of a PCM solar air heat exchanger and its ventilation preheating effectiveness,

Renew. Energy 145 (2020) 106–115, https://doi.org/10.1016/j.renene.2019.05.115.
[21] Y. Hu, P.K. Heiselberg, R. Guo, Ventilation cooling/heating performance of a PCM enhanced ventilated window - an experimental study, Energy Build. (2020), https://doi.org/10.1016/j.enbuild.2020.109903.
[22] Y. Hu, R. Guo, P.K. Heiselberg, Performance and control strategy development of a PCM enhanced ventilated window system by a combined experimental and numerical study, Renew. Energy 155 (2020) 134–152, https://doi.org/10.1016/j.renene.2020.03.137.
[23] E. Solgi, Z. Hamedani, R. Fernando, B. Mohammad Kari, H. Skates, A parametric study of phase change material behaviour when used with night ventilation in different climatic zones, Build. Environ. 147 (2019) 327–336, https://doi.org/10.1016/j.buildenv.2018.10.031.
[24] G. Cao, H. Awbi, R. Yao, Y. Fan, K. Sirén, R. Kosonen, J.(Jensen, Zhang, A review of the performance of different ventilation and airflow distribution systems in buildings, Build. Environ. 73 (2014) 171–186, https://doi.org/10.1016/j.buildenv.2013.12.009.
[25] S. Rahnama, P. Sadeghian, P.V. Nielsen, C. Zhang, S. Sadrizadeh, A. Afshari, Cooling capacity of diffuse ceiling ventilation system and the impact of heat load and diffuse panel distribution, Build. Environ. 185 (2020) 107290, https://doi.org/10.1016/j.buildenv.2020.107290.
[26] C. Zhang, T. Yu, P. Heiselberg, M. Pominaowski, P. Nielsen, Diffuse Ceiling Ventilation – Design Guide, 2016 accessed, https://vbn.aau.dk/ws/portalfiles/portal/243057526/Diffuse_ceiling_ventilation_Design_guide.pdf. (Accessed 5 June 2019).
[27] C.A. Hviid, S. Petersen, Integrated ventilation and night cooling in classrooms with diffuse ceiling ventilation, in: 11Th Ökosan, 2011 accessed, https://orbit.dtu.dk/en/publications/integrated-ventilation-and-night-cooling-in-classrooms-with-diffu. (Accessed 30 October 2020).
[28] C.A. Hviid, J. Lessing, Experimental study of the heat transfers and passive cooling potential of a ventilated plenum designed for uniform air distribution, in: 12th REHVA World Congr, CLIMA, 2016. https://orbit.dtu.dk/en/publications/experimental-study-of-the-heat-transfers-and-passive-cooling-pote.
[29] W. Wu, N. Yoon, Z. Tong, Y. Chen, Y. Lv, T. Ærenlund, J. Benner, Diffuse ceiling ventilation for buildings: a review of fundamental theories and research methodologies, J. Clean. Prod. 211 (2019) 1600–1619, https://doi.org/10.1016/j.jclepro.2018.11.148.
[30] T. Yu, P. Heiselberg, B. Lei, M. Pomianowski, C. Zhang, A novel system solution for cooling and ventilation in office buildings: a review of applied technologies and a case study, Energy Build. 90 (2015) 142–155, https://doi.org/10.1016/j.enbuild.2014.12.057.
[31] B. Yang, A.K. Melikov, A. Kabanshi, C. Zhang, F.S. Bauman, G. Cao, H. Awbi, H. Wigö, J. Niu, K.W.D. Cheong, K.W. Tham, M. Sandberg, P.V. Nielsen, R. Kosonen, R. Yao, S. Kato, S.C. Sekhar, S. Schiavon, T. Karimipanah, X. Li, Z. Lin, A review of advanced air distribution methods - theory, practice, limitations and solutions, Energy Build. 202 (2019) 109359, https://doi.org/10.1016/j.enbuild.2019.109359.
[32] R. Guo, P. Heiselberg, Y. Hu, H. Johra, C. Zhang, R.L. Jensen, K.T. Jønsson, P. Peng, Experimental investigation of convective heat transfer for night cooling with diffuse ceiling ventilation, Build. Environ. 193 (2021) 107665, https://doi.org/10.1016/j.buildenv.2021.107665.
[33] R. Guo, P. Heiselberg, Y. Hu, H. Johra, R.L. Jensen, K.T. Jønsson, P. Peng, Experimental investigation of convective heat transfer for night ventilation in case of mixing ventilation, Build. Environ. 193 (2021) 107670, https://doi.org/10.1016/j.buildenv.2021.107670.
[34] P. Roach, F. Bruno, M. Belusko, Modelling the cooling energy of night ventilation and economiser strategies on façade selection of commercial buildings, Energy Build. 66 (2013) 562–570, https://doi.org/10.1016/j.enbuild.2013.06.034.
[35] Z. Wang, L. Yi, F. Gao, Night ventilation control strategies in office buildings, Sol. Energy 83 (2009) 1902–1913, https://doi.org/10.1016/j.solener.2009.07.003.
[36] M. Kolokotroni, A. Aronis, Cooling-energy reduction in air-conditioned offices by using night ventilation, Appl. Energy 63 (1999) 241–253, https://doi.org/10.1016/S0306-2619(99)00031-8.
[37] E. Solgi, R. Fayaz, B.M. Kari, Cooling load reduction in office buildings of hot-arid climate, combining phase change materials and night purge ventilation, Renew. Energy 85 (2016) 725–731, https://doi.org/10.1016/j.renene.2015.07.028.
[38] C. Piselli, M. Prabhakar, A. de Gracia, M. Saffari, A.L. Pisello, L.F. Cabeza, Optimal control of natural ventilation as passive cooling strategy for improving the energy performance of building envelope with PCM integration, Renew. Energy 162 (2020) 171–181, https://doi.org/10.1016/j.renene.2020.07.043.
[39] R. Guo, Y. Gao, C. Zhuang, P. Heiselberg, R. Levinson, X. Zhao, D. Shi, Optimization of cool roof and night ventilation in office buildings: a case study in Xiamen, China, Renew. Energy 147 (2020) 2279–2294, https://doi.org/10.1016/j.renene.2019.10.032.
[40] R. Guo, P. Heiselberg, Y. Hu, C. Zhang, S. Vasilevskis, Optimization of night ventilation performance in office buildings in a cold climate, Energy Build. 225 (2020) 110319, https://doi.org/10.1016/j.enbuild.2020.110319.
[41] N. Bureau Of Standards, Thermal Analysis Research Program Reference Manual, 1983.
[42] D.E. Fisher, C.O. Pedersen, Convective heat transfer in building energy and thermal load calculations, ASHRAE Trans 103 (1997) 137–148. https://citeseerx.ist.psu.edu/viewdoc/download?doi=10.1.1.616.9820&rep=rep1&type=pdf.
[43] U.S. Department of Energy, EnergyPlus 9.3 input output reference. https://bigladdersoftware.com/epx/docs/9-3/input-output-reference/, 2020.
[44] Global Mathworks, Optimization Toolbox, User's Documentation R2019b, The MathWorks Inc., Massachusetts, 2019. https://www.mathworks.com/help/gads/index.
[45] EN 15251, Indoor Environmental Input Parameters for Design and Assessment of Energy Performance of Buildings Addressing Indoor Air Quality, Thermal Environment, Lighting and Acoustics, 2007. https://webshop.ds.dk/Default.aspx?ID=219&GroupID=91.040.01&ProductID=M204572.
[46] ISO 7730:2005 - Ergonomics of the Thermal Environment — Analytical Determination and Interpretation of Thermal Comfort Using Calculation of the PMV and PPD Indices and Local Thermal Comfort Criteria, 2005. https://www.iso.org/standard/39155.html.
[47] WMO Country Profile Database, World meteorological organization. https://www.wmo.int/cpdb/, 2018.
[48] S. Petersen, N.U. Christensen, C. Heinsen, A.S. Hansen, Investigation of the displacement effect of a diffuse ceiling ventilation system, Energy Build. 85 (2014) 265–274, https://doi.org/10.1016/j.enbuild.2014.09.041.
[49] X. Tian, B. Li, Y. Ma, D. Liu, Y. Li, Y. Cheng, Experimental study of local thermal comfort and ventilation performance for mixing, displacement and stratum ventilation in an office, Sustain. Cities Soc. 50 (2019) 101630, https://doi.org/10.1016/j.scs.2019.101630.
[50] International Energy Agency, Technical Note AIVC 65 - Recommendations on Specific Fan Power and Fan System Efficiency, 2009. https://www.aivc.org/sites/default/files/members_area/medias/pdf/Technotes/TN65_Specific Fan Power.pdf.
[51] P. Filipsson, A. Trüschel, J. Gräslund, J.O. Dalenbäck, Modelling of rooms with active chilled beams, J. Build. Perform. Simul. 13 (2020) 409–418, https://doi.org/10.1080/19401493.2020.1752801.
[52] K. Goldstein, A. Novoselac, Convective heat transfer in rooms with ceiling slot diffusers (rp-1416), HVAC R Res. 16 (2010) 629–655, https://doi.org/10.1080/10789669.2010.10390925.
[53] C. Zhuang, K. Shan, S. Wang, Coordinated demand-controlled ventilation strategy for energy-efficient operation in multi-zone cleanroom air-conditioning systems, Build. Environ. 191 (2021) 107588, https://doi.org/10.1016/j.buildenv.2021.107588.
[54] C. Zhuang, Y. Gao, Y. Zhao, R. Levinson, P. Heiselberg, Z. Wang, R. Guo, Potential benefits and optimization of cool-coated office buildings: a case study in Chongqing, China, Energy 226 (2021) 120373, https://doi.org/10.1016/j.energy.2021.120373.
[55] U.S. Department of Energy, EnergyPlus 9.3 auxiliary programs. https://bigladdersoftware.com/epx/docs/9-3/auxiliary-programs/index.html, 2020.
[56] Mathworks, Parallel Computing Toolbox, User's Documentation R2019b, The MathWorks Inc., Massachusetts, 2019. https://www.mathworks.com/help/parallel-computing/index.
[57] A. Ebrahimi-Moghadam, P. Ildarabadi, K. Aliakbari, F. Fadaee, Sensitivity analysis and multi-objective optimization of energy consumption and thermal comfort by using interior light shelves in residential buildings, Renew. Energy 159 (2020) 736–755, https://doi.org/10.1016/j.renene.2020.05.127.